Analytical Solution of Scattering by a 2D Dielectric Filled Crack in a Ground Plane Coated by a Dielectric Layer: TE Case

B. Ghalamkari [1], A Tavakoli [1, 2], and M. Dehmollaian[3]

[1] Department of Electrical Engineering
[2]Institute of Communications Technology and Applied Electromagnetics
Amirkabir University of Technology, Tehran, 15914, Iran
B.Ghalamkari@aut.ac.ir,Tavakoli@aut.ac.ir

[3] Department of Electrical and Computer Engineering
University of Tehran, Tehran, 14395-515, Iran
M.Dehmollaian@ece.ut.ac.ir

Abstract ─ Analytical solution of scattering by a 2D loaded crack on a ground plane, coated by a dielectric layer for TE case is studied theoretically using Kobayashi and Nomura's (Kobayashi Potential) method. The geometry is divided into three regions whose fields are expressed in terms of Bessel eigenfunctions. The problem is reduced to a system of equations involving truncated summations with an infinite number of unknowns. Excitation coefficients are determined by applying the boundary conditions. By applying Weber-Schafheitlin discontinuous integrals, the infinite summations could efficiently be truncated with high numerical accuracy. For validation, in addition to convergence analysis, near-field magnetic current densities on the crack and the radar cross section (RCS) results are compared with those of Finite Element Method (FEM). Having the analytical method, the influence of the filling and the dielectric layer is investigated.

Index Terms - Plane wave scattering, 2D coated crack, dielectric layer, Kobayashi and Nomura method, Weber-Schafheitlin discontinuous integrals.

I. INTRODUCTION

Crack detection is one of the important tasks in nondestructive testing (NDT) of industrial materials and products. Near-field microwave resonator [1] and waveguide techniques [2], [3] have been utilized to detect surface cracks on metals. For non-accessible cracks like those on boilers or blast furnaces, far-field electromagnetic (EM) scattering measurement is recommended [4-18].

The solution of EM scattering by a narrow and arbitrary shaped gap was given by Senior et al. using a point matching method of moment (MoM) [19]. Barkeshli and Volakis have applied the equivalence principal to obtain the equivalent current on the aperture for a quasi static solution [20]. Park et al. formulated the scattering problem for a rectangular crack in a spectral Fourier spectrum domain [21]. Jin used finite element method (FEM) for inside the crack and boundary integral (BI) for field over a perfect electric conductor (PEC) plane [22]. The natural frequency poles extraction with matrix pencil method (MPM) is also given by Deek et al. for detecting cracks in buried pipes [23]. Bozorgi, et al. presented a direct modeling technique based on field integral equation (FIE) for determining the back scattering signatures of a crack in a metallic surface by removing singularities in hypersingular integrals [4, 5]. Honarbakhsh and Tavakoli introduced meshfree collocation method to solve 2D filled cracks in PEC [24]. Other techniques that have been used to solve similar geometries include overlapping T-block method [13-16] transparent boundary condition (TBC) [17] and mode expansion scattering solution for wide rectangular cracks in 2D [25] and cavities in 3D [26].

The Kobayashi potential (KP) method has also been used in various EM scattering problems [6-12]. This method is applicable to all geometrical cracks for TE and TM cases.

Submitted On: June 10, 2012
Accepted On: Aug. 22, 2012

The KP method has some simplifying advantages compared to other numerical techniques (mainly MoM). First, the KP method is accurate and simple in the sense of not dealing with singularity of the Green's functions. Second, since each function involved in the integrand of the potential functions satisfies a part of required boundary conditions, solutions converge rapidly [7].

Sato and Shirai utilized KP method to analyze EM plane wave scattering by a 2D filled rectangular crack on a ground plane without any dielectric coating [9]. They applied the standard impedance boundary condition (SIBC) [10] and estimated the depth of the crack [11]. They also applied KP method to model the propagation through slits array [12].

Since paint, rust, and oil coatings on cracks alter the scattering signature, a solution that takes the dielectric coating effect into consideration is in demand for practical purposes. Here, EM plane wave scattering by a 2D gap in a PEC ground plane coated by a dielectric layer is analyzed. The scattered field is rigorously formulated using the KP method.

The paper is organized as follows. In section II, standing waves in the paint layer are formulated. The KP method is utilized to derive the governing field equations with unknown excitation coefficients in section III. In section IV, the truncated unknown excitation coefficients are computed. The numerical results and validations are presented in section V.

We assumed a time dependence of $e^{-i\omega t}$ throughout the context.

II. THE SCATTERING PROBLEM WITHOUT CRACK

The geometry of a slab of height y_t and relative permittivity of ε_1 and relative permeability of μ_1 on an infinite PEC ground plane is depicted in Fig. 1.

Here, $k_0 = \omega\sqrt{\varepsilon_0\mu_0}$ and $k_1 = k_0\sqrt{\varepsilon_1\mu_1}$ are respectively the free space and the dielectric slab wave numbers. The slab is illuminated by a vertically polarized EM plane wave:

$$\phi^i\left(=H_z^i\right)=e^{-ik_0(x\cos\theta_0+y\sin\theta_0)}, \tag{1}$$

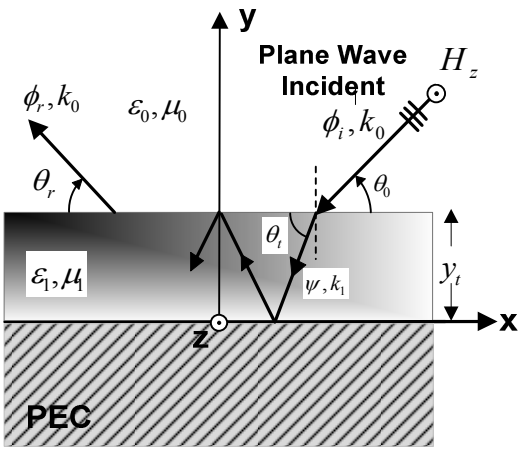

Fig. 1. Geometry of an infinite ground plane coated with a slab.

and the reflected plane wave is:

$$\phi^r\left(=H_z^r\right)=\mathrm{Re}^{-ik_0(x\cos\theta_0-y\sin\theta_0)}, \tag{2}$$

where, R is the reflection coefficient, θ_0 is the incident angle, θ_t is the transmission angle, and θ_r is the reflection angle. Assuming ψ is the total magnetic field in dielectric slab. Thus,

$$\psi=\left[Ae^{-ik_1\sin\theta_t(y-y_t)}+Be^{+ik_1\sin\theta_t y}\right]e^{-ik_1\cos\theta_t x}, \tag{3}$$

Where A and B are unknown coefficients. The first term in (3) represents the down-going and the second term is the up-going wave.

In order to find the aforementioned unknowns first, we note that the tangential field component $E_x=-\frac{1}{i\omega\varepsilon}\frac{\partial\psi}{\partial y}$ is zero over the PEC boundary $(y=0)$ therefore:

$$B=Ae^{ik_1y_t\sin\theta_t}, \tag{4}$$

Second, imposing the continuity of the tangential field components H_z and E_x at $y=y_t$ yields:

$$e^{-ik_0y_t(\sin\theta_0)}+\mathrm{Re}^{ik_0y_t(\sin\theta_0)}=A\left[1+e^{ik_1 2y_t(\sin\theta_t)}\right], \tag{5}$$

$$\left(-\frac{1}{\varepsilon_0}e^{-ik_0y_t(\sin\theta_0)}+\frac{R}{\varepsilon_0}e^{ik_0y_t(\sin\theta_0)}\right)\left(ik_0\sin\theta_0\right)=$$

$$\frac{A}{\varepsilon_0\varepsilon_1}\left(ik_1\sin\theta_t\right)\left[-1+e^{ik_1 2y_t(\sin\theta_t)}\right]. \tag{6}$$

By solving (5) and (6) simultaneously, we get

$$A=\frac{2e^{-ik_0y_t(\sin\theta_0)}}{1+\dfrac{k_1\sin\theta_t}{\varepsilon_1k_0\sin\theta_0}+e^{ik_1 2y_t(\sin\theta_t)}\left[1-\dfrac{k_1\sin\theta_t}{\varepsilon_1k_0\sin\theta_0}\right]}, \quad (7)$$

$$R=\frac{-\dfrac{k_1\sin\theta_t}{\varepsilon_1k_0\sin\theta_0}\left[-1+e^{ik_1 2y_t(\sin\theta_t)}\right]-1-e^{ik_1 2y_t(\sin\theta_t)}}{\dfrac{k_1\sin\theta_t}{\varepsilon_1k_0\sin\theta_0}\left[-1+e^{ik_1 2y_t(\sin\theta_t)}\right]-1-e^{ik_1 2y_t(\sin\theta_t)}} .e^{-ik_0 2y_t(\sin\theta_0)}. \quad (8)$$

Thus, the magnetic field in dielectric slab can be expressed as:

$$\psi=A\left[e^{-ik_1(y-y_t)\sin\theta_t}+e^{+ik_1(y+y_t)\sin\theta_t}\right]e^{-ik_1\cos\theta_t x}. \quad (9)$$

where A is given in (7).

III. THE SCATTERING PROBLEM WITH CRACK

After deriving ψ, a dielectric filled rectangular crack of width $w=2a$ and depth b is assumed in the geometry, as shown in Fig. 2. The crack is assumed to be filled by a material with relative permittivity and permeability of ε_r and μ_r respectively. The filling and coating materials could be both lossy, meaning that $\varepsilon_r,\mu_r,\varepsilon_1$ and μ_1 could be complex.

Three distinctive regions are recognized here:

I) Semi-infinite half space $(y>y_t)$.

II) Slab region $(y_t>y>0)$.

III) Cavity region $(-b\le y<0,|x|<a)$.

We now derive the field representations in each region. The total z-component of the magnetic field and the additional scattering contribution of the crack are denoted by $\phi_i^t(i=1,2,3)$ and $\phi_i^s(i=1,2)$, respectively. Where the subscript i represents the region. In each region, the field is expanded over an appropriate Bessel eigenfunctions. The total fields in regions I and II are

$$\phi_1^t=\phi^i+\phi^r+\phi_1^s, \quad (10)$$

and

$$\phi_2^t=\psi+\phi_2^s. \quad (11)$$

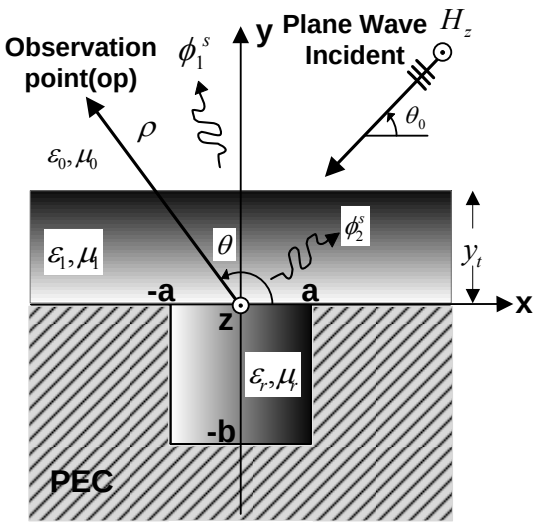

Fig. 2. Geometry of the filled rectangular crack underneath a coating layer in an infinite ground plane.

Additionally, since the scattered fields satisfy the homogeneous Helmholtz equation, utilizing the method of separation of variables, they could be represented as an integral of the general solutions [9]. Thus,

$$\phi_1^s=\frac{1}{a}\int_0^\infty\{d(\xi/a)\cos(\xi u)+e(\xi/a)\sin(\xi u)\}e^{-v\sqrt{\xi^2-\kappa_0^2}}d\xi. \quad (12)$$

and

$$\phi_2^s=\frac{1}{a}\int_0^\infty\{f(\xi/a)\cos(\xi u)+g(\xi/a)\sin(\xi u)\}e^{-v\sqrt{\xi^2-\kappa_1^2}}d\xi + \frac{1}{a}\int_0^\infty\{h(\xi/a)\cos(\xi u)+k(\xi/a)\sin(\xi u)\}e^{(v-t)\sqrt{\xi^2-\kappa_1^2}}d\xi. \quad (13)$$

where $d(.),e(.),f(.),g(.),h(.)$ and $k(.)$ are unknown weighting functions. In (12) and (13) normalized variables and parameters with respect to the half aperture width a are introduced as:

$$u=\frac{x}{a},v=\frac{y}{a},k_0=\frac{\kappa_0}{a},k_1=\frac{\kappa_1}{a},t=\frac{y_t}{a}. \quad (14)$$

It is worth mentioning that ϕ_1^s contains only an up-going wave while the first term of ϕ_2^s is an up-going wave and the second term is a down-going wave. Now, using

$$\begin{cases}\cos(\xi u)=\sqrt{\dfrac{\pi\xi u}{2}}J_{-1/2}(\xi u),\\ \sin(\xi u)=\sqrt{\dfrac{\pi\xi u}{2}}J_{1/2}(\xi u).\end{cases} \tag{15}$$

the weighting functions can be expanded over Bessel functions. Thus,

$$\begin{Bmatrix}d\\f\\h\end{Bmatrix}(\xi/a)=\sum_{m=0}^{\infty}\begin{Bmatrix}D_m\\F_m\\H_m\end{Bmatrix}\frac{J_{2m}(\xi)}{\sqrt{\xi^2-\kappa_0^2}}a, \tag{16}$$

And

$$\begin{Bmatrix}e\\g\\k\end{Bmatrix}(\xi/a)=\sum_{m=0}^{\infty}\begin{Bmatrix}E_m\\G_m\\K_m\end{Bmatrix}\frac{J_{2m+1}(\xi)}{\sqrt{\xi^2-\kappa_0^2}}a. \tag{17}$$

Substituting (15)-(17) into (12) and (13) yields:

$$\phi_1^s=\sqrt{\frac{\pi u}{2}}\sum_{m=0}^{\infty}\int_0^{\infty}\sqrt{\frac{\xi}{\xi^2-\kappa_0^2}}\begin{Bmatrix}D_mJ_{2m}(\xi)J_{-\frac{1}{2}}(\xi u)\\+E_mJ_{2m+1}(\xi)J_{\frac{1}{2}}(\xi u)\end{Bmatrix}$$
$$.e^{-v\sqrt{\xi^2-\kappa_0^2}}d\xi, \tag{18}$$

$$\phi_2^s=\sqrt{\frac{\pi u}{2}}\sum_{m=0}^{\infty}\int_0^{\infty}\sqrt{\frac{\xi}{\xi^2-\kappa_1^2}}\begin{Bmatrix}F_mJ_{2m}(\xi)J_{-\frac{1}{2}}(\xi u)\\+G_mJ_{2m+1}(\xi)J_{\frac{1}{2}}(\xi u)\end{Bmatrix}e^{-v\sqrt{\xi^2-\kappa_1^2}}d\xi$$
$$+\sqrt{\frac{\pi u}{2}}\sum_{m=0}^{\infty}\int_0^{\infty}\sqrt{\frac{\xi}{\xi^2-\kappa_1^2}}\begin{Bmatrix}H_mJ_{2m}(\xi)J_{-\frac{1}{2}}(\xi u)\\+K_mJ_{2m+1}(\xi)J_{\frac{1}{2}}(\xi u)\end{Bmatrix}e^{(v-t)\sqrt{\xi^2-\kappa_1^2}}d\xi. \tag{19}$$

Each component in the above integral expression is identified as a class of Weber-Schafheitlin type integral that automatically satisfy the zero tangential electric field boundary condition on a part of the ground plane where $|u|>1, v=0$.

The region III is like a parallel plate waveguide. Therefore, the field is expressed by a summation of waveguide modal eigenfunctions. Considering the boundary conditions at $x=\pm a$ and $y=-b$, ϕ_3^t is given by:

$$\phi_3^t=\sum_{n=0}^{\infty}L_n\left\{e^{-ih_nav}+e^{ih_na(v+2b_0)}\right\}\cos\left(\frac{n\pi}{2}(1-u)\right). \tag{20}$$

where $h_n=\sqrt{\varepsilon_r\mu_rk_0^2-(n\pi/w)^2}$ is the propagation constant for n th parallel plate waveguide mode, $b_0=\dfrac{b}{a}$ and L_n is an unknown coefficient.

IV. COMPUTATION OF THE UNKNOWN COEFFICIENTS

To determine the unknown coefficients D_m, E_m, F_m, G_m, H_m and K_m the continuity of the tangential field components $\phi^t(=H_z)$ and E_x at $y=0$ and $y=y_t$ are examined. Therefore,

$$\begin{cases}BC.1: at\ v=t(y=y_t)\ is\ \phi_1^s=\phi_2^s,\\ BC.2: at\ v=t(y=y_t)\ is\ \dfrac{\partial}{\partial v}\phi_1^s=\dfrac{\partial}{\varepsilon_1\partial v}\phi_2^s,\\ BC.3: at\ v=0(y=0)\ is\ \phi_2^t=\phi_3^t,\\ BC.4: at\ v=0(y=0)\ is\ \dfrac{\partial}{\varepsilon_1\partial v}\phi_2^t=\dfrac{\partial}{\varepsilon_r\partial v}\phi_3^t\end{cases} \tag{21}$$

By substituting *BC.1-4* and (15)-(17) in (18) and (19) and after some mathematical manipulation, the following equations are derived:

$BC.1$:

$$\sum_{m=0}^{\infty}\int_0^{\infty}\frac{1}{\sqrt{\xi^2-\kappa_0^2}}\begin{Bmatrix}D_mJ_{2m}(\xi)\cos(\xi u)\\+E_mJ_{2m+1}(\xi)\sin(\xi u)\end{Bmatrix}e^{-t\sqrt{\xi^2-\kappa_0^2}}d\xi$$
$$=\sum_{m=0}^{\infty}\int_0^{\infty}\frac{1}{\sqrt{\xi^2-\kappa_1^2}}\begin{Bmatrix}F_mJ_{2m}(\xi)\cos(\xi u)\\+G_mJ_{2m+1}(\xi)\sin(\xi u)\end{Bmatrix}e^{-t\sqrt{\xi^2-\kappa_1^2}}d\xi$$
$$+\sum_{m=0}^{\infty}\int_0^{\infty}\frac{1}{\sqrt{\xi^2-\kappa_1^2}}\begin{Bmatrix}H_mJ_{2m}(\xi)\cos(\xi u)\\+K_mJ_{2m+1}(\xi)\sin(\xi u)\end{Bmatrix}d\xi. \tag{22}$$

$BC.2$:

$$\varepsilon_1\sum_{m=0}^{\infty}\int_0^{\infty}\begin{Bmatrix}D_mJ_{2m}(\xi)\cos(\xi u)\\+E_mJ_{2m+1}(\xi)\sin(\xi u)\end{Bmatrix}e^{-t\sqrt{\xi^2-\kappa_0^2}}d\xi$$
$$=\sum_{m=0}^{\infty}\int_0^{\infty}\begin{Bmatrix}F_mJ_{2m}(\xi)\cos(\xi u)\\+G_mJ_{2m+1}(\xi)\sin(\xi u)\end{Bmatrix}e^{-t\sqrt{\xi^2-\kappa_1^2}}d\xi \tag{23}$$
$$-\sum_{m=0}^{\infty}\int_0^{\infty}\begin{Bmatrix}H_mJ_{2m}(\xi)\cos(\xi u)\\+K_mJ_{2m+1}(\xi)\sin(\xi u)\end{Bmatrix}d\xi.$$

$BC.3$:

$$\sum_{k=0}^{\infty}(-1)^k\begin{Bmatrix}L_{2k}\gamma_{2k}\cos(k\pi u)\\+L_{2k+1}\gamma_{2k+1}\sin\left(\dfrac{2k+1}{2}\pi u\right)\end{Bmatrix}=A2e^{ik_0y_i\sin\theta_i}e^{-ik_0x\cos\theta_0}$$
$$+\sum_{m=0}^{\infty}\int_0^{\infty}\frac{1}{\sqrt{\xi^2-\kappa_1^2}}\begin{Bmatrix}F_mJ_{2m}(\xi)\cos(\xi u)\\+G_mJ_{2m+1}(\xi)\sin(\xi u)\end{Bmatrix}d\xi$$
$$+\sum_{m=0}^{\infty}\int_0^{\infty}\frac{1}{\sqrt{\xi^2-\kappa_1^2}}\begin{Bmatrix}H_mJ_{2m}(\xi)\cos(\xi u)\\+K_mJ_{2m+1}(\xi)\sin(\xi u)\end{Bmatrix}e^{-t\sqrt{\xi^2-\kappa_1^2}}d\xi. \tag{24}$$

where $\gamma(.)=\left\{1+e^{ih(.)2ab_0}\right\}$.

$BC.4$:

$$\frac{\varepsilon_1}{\varepsilon_r}\sum_{k=0}^{\infty}(-1)^k\left\{\begin{matrix}L_{2k}(ih_{2k}a)\beta_{2k}\cos(k\pi u)\\+L_{2k+1}(ih_{2k+1}a)\beta_{2k+1}\sin\left(\frac{2k+1}{2}\pi u\right)\end{matrix}\right\}=$$

$$-\sum_{m=0}^{\infty}\int_0^{\infty}\left\{\begin{matrix}F_mJ_{2m}(\xi)\cos(\xi u)\\+G_mJ_{2m+1}(\xi)\sin(\xi u)\end{matrix}\right\}d\xi$$

$$+\sum_{m=0}^{\infty}\int_0^{\infty}\left\{\begin{matrix}H_mJ_{2m}(\xi)\cos(\xi u)\\+K_mJ_{2m+1}(\xi)\sin(\xi u)\end{matrix}\right\}e^{-t\sqrt{\xi^2-\kappa_1^2}}d\xi. \quad (25)$$

where $\beta(.)=\left\{-1+e^{ih(.)2ab_0}\right\}$.

These equations are solved by KP and then separated into odd and even groups using even and odd identities [6]. Thus:

$BC.1$: *Even Identity*:

$$\sum_{m=0}^{\infty}D_m\int_0^{\infty}J_{2m}(\xi)J_{2n}(\xi)\frac{e^{-t\sqrt{\xi^2-\kappa_0^2}}}{\sqrt{\xi^2-\kappa_0^2}}d\xi=$$

$$\sum_{m=0}^{\infty}F_m\int_0^{\infty}J_{2m}(\xi)J_{2n}(\xi)\frac{e^{-t\sqrt{\xi^2-\kappa_1^2}}}{\sqrt{\xi^2-\kappa_1^2}}d\xi+\sum_{m=0}^{\infty}H_m\int_0^{\infty}\frac{J_{2m}(\xi)J_{2n}(\xi)}{\sqrt{\xi^2-\kappa_1^2}}d\xi. \quad (26)$$

$BC.1$: *Odd Identity*:

$$\sum_{m=0}^{\infty}E_m\int_0^{\infty}J_{2m+1}(\xi)J_{2n+1}(\xi)\frac{e^{-t\sqrt{\xi^2-\kappa_0^2}}}{\sqrt{\xi^2-\kappa_0^2}}d\xi=$$

$$\sum_{m=0}^{\infty}G_m\int_0^{\infty}J_{2m+1}(\xi)J_{2n+1}(\xi)\frac{e^{-t\sqrt{\xi^2-\kappa_1^2}}}{\sqrt{\xi^2-\kappa_1^2}}d\xi+\sum_{m=0}^{\infty}K_m\int_0^{\infty}\frac{J_{2m+1}(\xi)J_{2n+1}(\xi)}{\sqrt{\xi^2-\kappa_1^2}}d\xi. \quad (27)$$

$BC.2$: *Even Identity*:

$$\varepsilon_1\sum_{m=0}^{\infty}D_m\int_0^{\infty}J_{2m}(\xi)J_{2n}(\xi)e^{-t\sqrt{\xi^2-\kappa_0^2}}d\xi=$$

$$\sum_{m=0}^{\infty}F_m\int_0^{\infty}J_{2m}(\xi)J_{2n}(\xi)e^{-t\sqrt{\xi^2-\kappa_1^2}}d\xi-\sum_{m=0}^{\infty}H_m\int_0^{\infty}J_{2m}(\xi)J_{2n}(\xi)d\xi. \quad (28)$$

$BC.2$: *Odd Identity*:

$$\varepsilon_1\sum_{m=0}^{\infty}E_m\int_0^{\infty}J_{2m+1}(\xi)J_{2n+1}(\xi)e^{-t\sqrt{\xi^2-\kappa_0^2}}d\xi=$$

$$\sum_{m=0}^{\infty}G_m\int_0^{\infty}J_{2m+1}(\xi)J_{2n+1}(\xi)e^{-t\sqrt{\xi^2-\kappa_1^2}}d\xi-\sum_{m=0}^{\infty}K_m\int_0^{\infty}J_{2m+1}(\xi)J_{2n+1}(\xi)d\xi. \quad (29)$$

$BC.3$: *Even Identity*:

$$\sum_{k=0}^{\infty}(-1)^k\left\{L_{2k}\gamma_{2k}J_{2n}(k\pi)\right\}=2Ae^{jk_{y_i}\sin\theta_i}J_{2n}(\kappa_0\cos\theta_0)$$

$$+\sum_{m=0}^{\infty}F_m\int_0^{\infty}\frac{J_{2m}(\xi)J_{2n}(\xi)}{\sqrt{\xi^2-\kappa_1^2}}d\xi+\sum_{m=0}^{\infty}H_m\int_0^{\infty}J_{2m}(\xi)J_{2n}(\xi)\frac{e^{-t\sqrt{\xi^2-\kappa_1^2}}}{\sqrt{\xi^2-\kappa_1^2}}d\xi. \quad (30)$$

$BC.3$: *Odd Identity*:

$$\sum_{k=0}^{\infty}(-1)^k\left\{L_{2k+1}\gamma_{2k+1}J_{2n+1}\left(\frac{2k+1}{2}\pi\right)\right\}=-2iAe^{jk_{y_i}\sin\theta_i}J_{2n+1}(\kappa_0\cos\theta_0)$$

$$+\sum_{m=0}^{\infty}G_m\int_0^{\infty}\frac{J_{2m+1}(\xi)J_{2n+1}(\xi)}{\sqrt{\xi^2-\kappa_1^2}}d\xi+\sum_{m=0}^{\infty}K_m\int_0^{\infty}J_{2m+1}(\xi)J_{2n+1}(\xi)\frac{e^{-t\sqrt{\xi^2-\kappa_1^2}}}{\sqrt{\xi^2-\kappa_1^2}}d\xi. \quad (31)$$

$BC.4$: *Even Identity*:

$$\frac{\varepsilon_1}{\varepsilon_r}L_{2k}(-1)^k(ih_{2k}a)\beta_{2k}(\delta_{0k}+1)=\pi\sum_{m=0}^{\infty}J_{2m}(k\pi)\left\{\begin{matrix}(-1)F_m\\e^{-t\sqrt{(k\pi)^2-\kappa_1^2}}H_m\end{matrix}\right\}. \quad (32)$$

where δ_{mk} is the Kronecker delta.

$BC.4$: *Odd Identity*:

$$\frac{\varepsilon_1}{\varepsilon_r}L_{2k+1}(-1)^k(ih_{2k+1}a)\beta_{2k+1}=\pi\sum_{m=0}^{\infty}J_{2m+1}\left(\frac{2k+1}{2}\pi\right)\left\{\begin{matrix}(-1)G_m\\e^{-t\sqrt{\left(\frac{2k+1}{2}\pi\right)^2-\kappa_1^2}}K_m\end{matrix}\right\}. \quad (33)$$

Equations (26)-(33) are eight sets of equations to solve eight sets of unknown coefficients D_m, E_m, F_m, G_m, H_m, K_m, L_{2k}, L_{2k+1}.

In a cylindrical coordinate system where the observation point is represented by ρ and θ the far-field scattering is [11]:

$$\phi_1^s=\sqrt{\frac{\pi}{2k_0\rho}}e^{i_1\left(k_0\rho+\pi/4\right)}\sum_{m=0}^{\infty}\left\{\begin{matrix}D_mJ_{2m}\left(k_0a\cos\theta\right)\\-iE_mJ_{2m+1}\left(k_0a\cos\theta\right)\end{matrix}\right\}. \quad (34)$$

The above summations are all convergent and therefore, n and m are limited to N and M, respectively.

V. NUMERICAL RESULTS AND VALIDATION

In this section, the proposed analytical method is applied to several coated cracks and validated by three approaches. First, FEM is used to find $\phi_3^t\left(=H_z^t\right)$ and the magnetic current densities M_x, on the aperture for different incident angles. Second, the RCS is computed by exploiting the coated ground Green's function together with the near to far-field transformation [27]. Third, for rigorous validation of the method, convergence analysis curves are provided [28]. The studied scenarios of the crack cases are listed in Table 1.

A. Validation with magnetic current density analysis

Referring to Fig. 2 and Table 1, in case A only the permittivity of the coating layer is complex whereas in case B all filling and coating materials are complex. The calculated magnetic current density distributions $|M_x|$ on the crack $(|x|<a,\ y=0)$ at various incident angles $(\theta_0=15°, 30°, 45°, 60°, 75°, 90°)$ are shown in Fig.

3 where $N = M = 13$. Comparison of the results with the FEM solution demonstrates the accuracy of the method at all incident angles.

Table 1: Different scenarios of cracks

	w	b	ε_r	μ_r	ε_1	μ_1	y_t
A	$0.2\lambda_0$	$0.2\lambda_0$	1	1	$2+0.1i$	1	$\lambda_0/10$
B	$0.2\lambda_0$	$0.2\lambda_0$	$2.5+0.2i$	$1.8+0.1i$	$2+0.1i$	$1.5+0.2i$	$\lambda_0/10$
C	$1\lambda_0$	$0.2\lambda_0$	$2.5+0.2i$	1	2	1	$\lambda_0/7$
D	$1\lambda_0$	$0.2\lambda_0$	$4+0.2i$	1	3	1	$\lambda_0/7$
E [9]	$2\lambda_0$	$0.5\lambda_0$	$2.5+0.2i$	$1.8+0.1i$	---	---	---
F	$2\lambda_0$	$0.5\lambda_0$	$2.5+0.2i$	$1.8+0.1i$	$3.2+0.1i$	$1.6+0.2i$	$\lambda_0/5$
G [22]	2.5 *cm*	1.25 *cm*	1	1	---	---	---
H	$1.5\lambda_0$	$10\lambda_0$	$2.7+0.03i$	$1.4+0.1i$	---	---	---

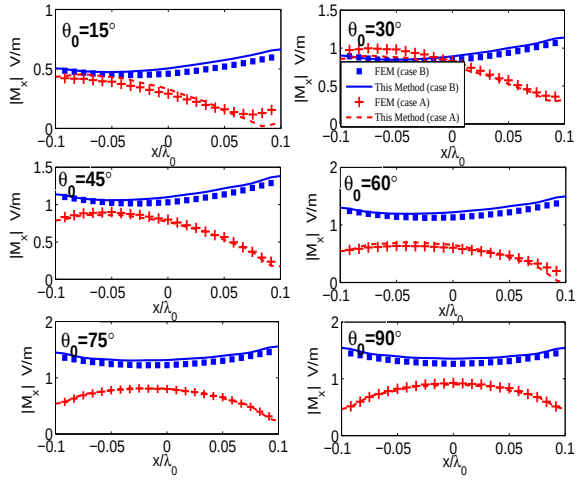

Fig. 3. Magnetic current densities on the crack $(|x| < a,\ y = 0)$ computed by the proposed method and FEM for cases A and B.

B. Validation with RCS analysis

For cases C and D, normalized RCS as a function of incident angle is depicted in Fig. 4. with $N = M = 11$. The results are compared to FEM solution. Here, the width of the crack is $w = 1\lambda_0$ to show the applicability of this method for wide cracks.

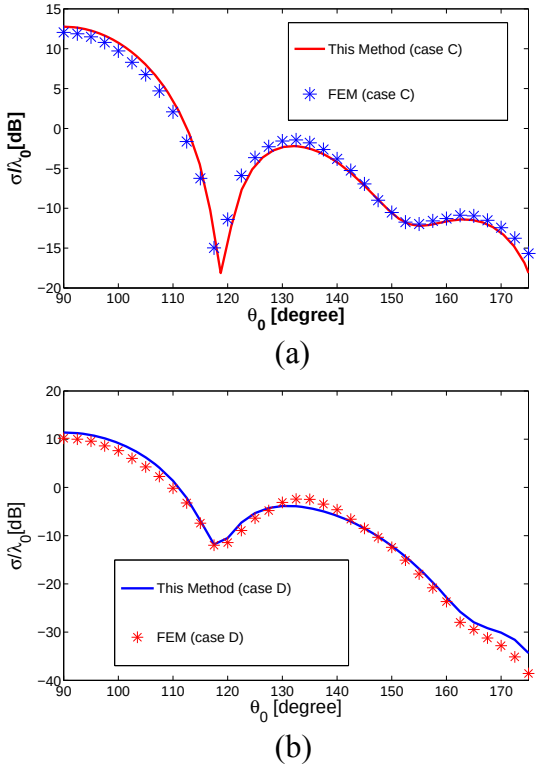

Fig. 4. Normalized RCS as a function of incident angles for (a) case C and (b) case D.

C. Validation with convergence analysis

For error analysis, the convergence curves for cases A, E and F where $\theta_0 = 90^\circ$ are represented in Fig. 5. The error function and Euclidean norm are given by:

$$\begin{cases} e_r = \left\| M^{i+1}_{x_k} - M^{i}_{x_k} \right\| \Big/ \left\| M^{i}_{x_k} \right\|, \ i = 1..N, \\ \left\| M^{i}_{x_k} \right\| = \sqrt{\sum_{k=1}^{K} \left| M^{i}_{x_k} \right|^2}. \end{cases} \quad (34)$$

where x_k is the position of the k th point on the crack and K is the total number of observation points. The results are calculated using $K = 25$ for all three cases.

As mentioned before, Weber-Schafheitlin type integrals automatically satisfy the boundary condition on the PEC $(|x| > a, v = 0)$ and the summations converge very rapidly. Referring to

Fig. 5, for a N close to 12~14, we have the error of $10^{-2.2} = 0.00631$. The rapid convergence of this analytic method makes it desirable for efficient calculation of the scattered field in inverse problems.

D. Results

Here, the reported backscattered results of a crack with the dielectric cover and without the dielectric cover of [9, 22, 24] are compared to the proposed method. In Fig. 6 (a), the normalized RCS of case E (without a coating layer) is compared with that reported in [9]. In addition, by imposing a thin layer on the crack (case F), the influence on the RCS is evident. In addition, our proposed method could also be applied to narrow cracks. Figure 6 (b) shows the normalized RCS of the case H that is a very narrow crack with and without a coating layer. The coating is a $\lambda_0/8$ layer of paint primer ($\varepsilon_1 = 3.48 + 0.12i$). According to Fig. 6, RCS drops down at grazing angles for coated cracks.

Figure 7 shows the normalized RCS as a function of frequency for open crack at a low grazing angle of $\theta_0 = 10^\circ$ (case G). Here, results of finite element boundary integral method (FE-BI) and measurements of [22], meshfree method (MFM) [24] and our method are compared with each other. A good agreement is observed between these methods. Since these solutions do not consider the coating layer, the same case with a 2mm layer of common paint with a relative dielectric constant $\varepsilon_1 = 3 + 0.1i$ [3] is also simulated. Solid line with diamonds in Fig. 7 depicts the results of presented method. Examination of the results shows that the crack dielectric cover alter the RCS signature significantly.

Figures 8 and 9 depict the variation of normalized RCS for various materials of Table 2 for a crack of $w = 0.2\lambda_0$, $b = 0.2\lambda_0$, $\mu_1 = \mu_r = 1$ and $\theta_0 = 90^\circ$. In addition, the cracks in all cases are filled by rust with $\varepsilon_r = 2.7 + 0.03i$.

By increasing the dielectric constant and hence the electrical depth, RCS drops down at first and then increases due to an increase in the electrical thickness of the substrate that excites additional surface wave modes. By increasing the paint depth, the term ψ bounces in slab and its energy decreases. Therefore, RCS reduces as paint depth increases. Additionally, when the coating is lossy, the RCS is significantly affected for even low loss as shown in Fig. 9. Normalized RCS of the crack versus the paint depth for various amount of permeability is shown in Fig. 10. assuming a crack with $w = 0.2\lambda_0$, $b = 0.2\lambda_0$, $\varepsilon_r = 2.7 + 0.03i$ and $\theta_0 = 90^\circ$.

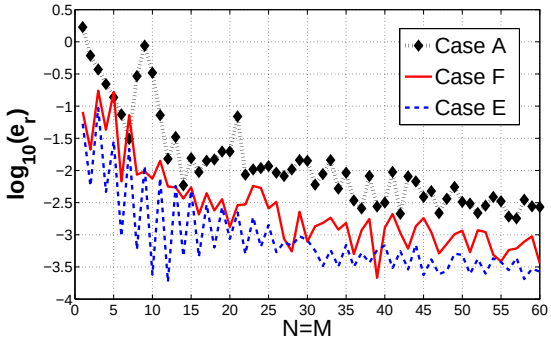

Fig. 5. Convergence curves for cases A, E and F.

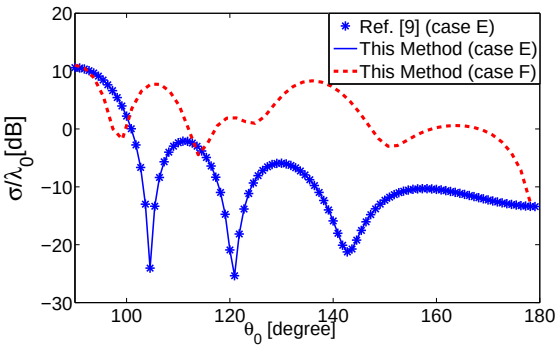

(a)

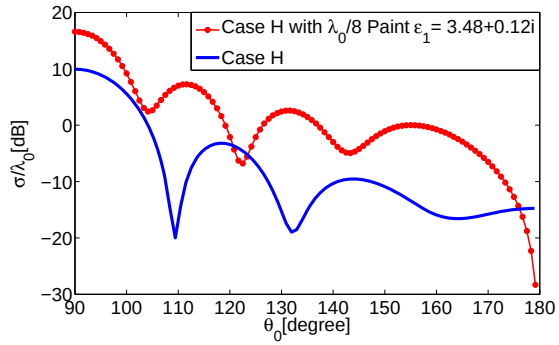

(b)

Fig. 6. Normalized RCS as a function of incident angles for (a) case E[9], and with a dielectric layer of case F (b) case H, and with a $\lambda_0/8$ dielectric layer of $\varepsilon_1 = 3.48 + 0.12i$.

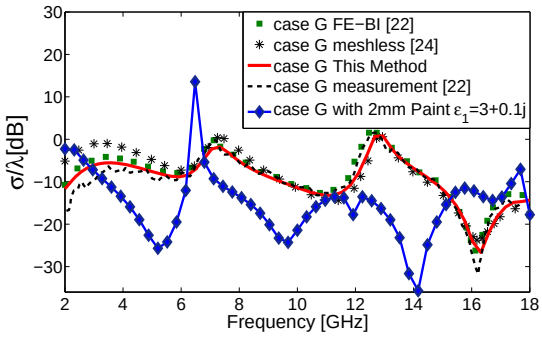

Fig. 7. Normalized RCS as a function of frequency for case G [22, 24] and with a 2mm dielectric layer of $\varepsilon_1 = 3 + 0.1i$ at a low grazing angle of $\theta_0 = 10^\circ$.

Table 2: Some coatings and their complex dielectric constants

Material	ε_r'	ε_r''
Fe_2O_3 Powder (Rust)	2.7	0.03i
Paint Primer	3.48	0.12i
Salt Rust	5.33	1.53i
Red Rust	8.42	1.03i

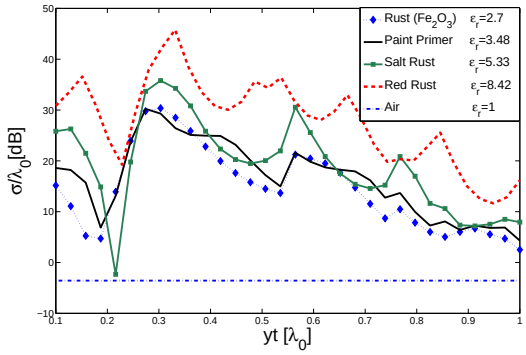

Fig. 8. Normalized RCS of the crack as a function of coating depth for different real dielectric constants where $w = 0.2\lambda_0$, $b = 0.2\lambda_0$, $\mu_1 = \mu_r = 1$, $\varepsilon_r = 2.7 + 0.03\,i$ and $\theta_0 = 90^\circ$.

VI. CONCLUSION

Paint layer on fatigue cracks play an important role in RCS results and thus crack detection as a state of the art in microwave NDT. In this paper, EM plane wave scattering by a 2D rectangular filled and coated crack on a ground plane is analyzed by KP method for TE case. In order to show the validity of the solution, three methods are used. The magnetic current on the aperture and RCS results compared with FEMs'. On the other hand, the approach and its efficiency are validated by convergence analysis. The method is shown to be accurate for both narrow and wide cracks. The proposed method is applicable to all lossy and lossless materials for filled and coated cracks. In addition, the sensitivity of the RCS to the permittivity, permeability and thickness of the overlaying layer is presented.

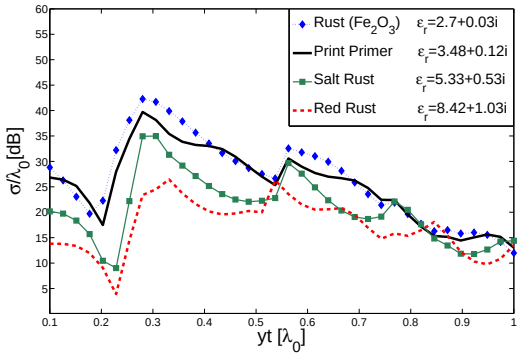

Fig. 9. Normalized RCS of the crack as a function of coating depth for different complex dielectric constants where $w = 0.2\lambda_0$, $b = 0.2\lambda_0$, $\mu_1 = \mu_r = 1$, $\varepsilon_r = 2.7 + 0.03\,i$ and $\theta_0 = 90^\circ$.

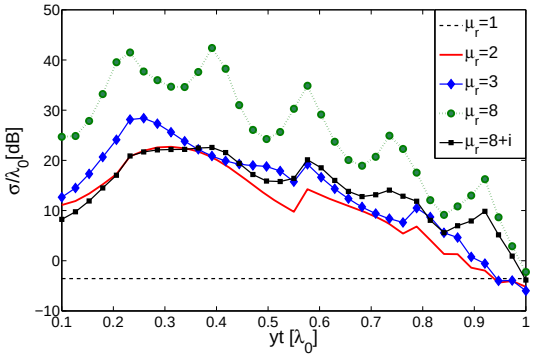

Fig. 10. Normalized RCS of the crack versus paint depth for different permeabilities for $w = 0.2\lambda_0$, $b = 0.2\lambda_0$, $\varepsilon_r = 2.7 + 0.03\,i$ and

ACKNOWLEDGMENT

The authors would like to thank Iran Telecommunication Research Center (ITRC) for supporting this work. The authors also appreciate

Prof. Shirai's of Chuo University for his valuable inputs.

REFERENCES

[1] J. Kerouedan, P. Queffelec, P. Talbot, C. Quendo, and A. L. Brun, "Detecting of Micro-cracks on Metal Surfaces Using Near Field Microwave Dual Behaviour Resonators," *Springer, New Developments and App. in Sen. Tech*, vol. 83, pp. 1-13, 2011.

[2] A. McClanahan, S. Kharkovsky, A. R. Maxon, R. Zoughi, and D. D. Palmer, "Depth Evaluation of Shallow Surface Cracks in Metals Using Rectangular Waveguides at Millimeter-Wave Frequencies," *IEEE Transaction on Instrumentation and Measurement*, vol. 59, no. 6, pp. 1693-1704, June 2010.

[3] N. Qaddoumi, A. Shroyer, and R. Zoughi, "Microwave Detection of Rust under Paint and Composite Laminates," *Taylor and Francis Journal: Research in Nondestructive Evaluation*, vol. 9, no. 4, pp. 201-212, 1997.

[4] M. Bozorgi and A. Tavakoli, "Backscattering From a Two Dimensional Rectangular Crack Using FIE," *IEEE Trans. Antennas Propag.*, vol. 58, no. 2, pp. 552-564, Feb. 2010.

[5] M. Bozorgi and A. Tavakoli, "Plorimetric Scattering From a 3-D Rectangular Crack in a PEC Covered by a Dielectric Layer," *Applied Computational Electromagnetics Society (ACES) Journal*, vol. 26, no. 6, pp. 502-510, June 2011.

[6] Y. Nomura and S. Katsura, "Diffraction of Electromagnetic Waves by Ribbon and Slit. I," *Journal of the physical society of Japan*, vol. 12, pp. 190-200, Feb. 1957.

[7] K. Hongo and Q. A. Naqvi, "Similarities Between Moment Method and Kobayashi Potential," Proceedings of the IEICE General Conference, Kusatsu, Japan, 2001.

[8] K. Hongo and H. Serizawa, "Diffraction of Electromagnetic Plane Wave by a Rectangular Plate and a Rectangular Whole in the Conducting Plate," *IEEE Trans. Antennas Propag.*, vol. 47, no. 6, pp. 1029-1041, June 1999.

[9] R. Sato and H. Shirai, "Electromagnetic Plane Wave Scattering by a Loaded Trough on a Ground Plane," *IEICE Trans. Electron*, vol. E77-C, no. 12, pp. 1983-1989, Dec 1994.

[10] R. Sato and H. Shirai, "EM Scattering Analysis by a Loaded Trough on a Ground Plane using SIBC-E Polarization Case," in *IEEE Antennas and Propagation Society Int. Symp. Digest,* pp. 2858-2861, Aug 1999.

[11] H. Shirai and H. Sekiguchi, "A Simple Crack Depth Estimation Method from Backscattering Response," *IEEE Trans. on Instrumentation and Measurement* vol. 53, no. 4, pp. 1249-1254, Aug 2004.

[12] R. Sato and H. Shirai, "Propagation Analysis for a Simplified Indoor/outdoor Interface Model," in *IEEE Antennas and Propagation Society Int. Symp. Digest, AP-S.*, Nigata, Japan, 2010.

[13] Y. H. Cho, "Transverse Magnetic Plane-wave Scattering Equations for Infinite and Semi-infinite Rectangular Grooves in a Conducting Plane," *IET Microwaves, Antennas & Propagation*, vol. 2, no. 7, pp. 704–710, March 2008.

[14] Y. H. Cho, "TE Scattering from Large Number of Grooves Using Green's Functions and Floquet Modes," in *IEEE Microwave Conference*. Korea-Japan, pp. 41- 44, Nov. 2007.

[15] Y. H. Cho, "TM Plane-Wave Scattering From Finite Rectangular Grooves in a Conducting Plane Using Overlapping T-Block Method," *IEEE Trans. on Antennas and Propagation*, vol. 54, no. 2, pp. 746-749, Feb 2006.

[16] Y. H. Cho, "TM Scattering from Finite Rectangular Grooves in a Conducting Plane using Overlapping T-block Analysis," in *IEEE/ACES Conf. on Wireless Commun. and Applied Computational Electromagnetic*, pp. 744-747, 3-7 April 2005.

[17] K. Du, "Two Transparent Boundary Conditions for the Electromagnetic Scattering from Two-Dimensional Overfilled Cavities," *Elsevier Journal of Computational Physics,* vol. 230, no. 15, pp. 5822–5835, July 2011.

[18] B. Alavikia and O. M. Ramahi, "Fundamental Limitation on the Use of Open-Region Boundary Conditions and Matched Layers to Solve the Problem of Gratings in Metallic Screens," *Applied Computational Electromagnetics Society (ACES) Journal*, vol. 25, no. 8, pp. 652-658, Aug. 2010.

[19] B. A. Senior, K. Sarabandi, and J. R. Natzke, "Scattering by a Narrow Gap," *IEEE Trans. Antennas Propag.*, vol. 38, no. 7, pp. 1102-1111, July 1990.

[20] K. Barkeshli and J. L. Volakis, "Scattering from Narrow Rectangular Filled Grooves " *IEEE Trans. Antennas Propag.*, vol. 39, no. 6, pp. 804-810, June 1991.

[21] T. J. Park, H. J. Eom, and K. Yoshitomi, "An Analysis of Transverse Electric Scattering from a Rectangular Channel in a Conducting Plane," *Radio Science*, vol. 28, no. 5, pp. 663-673, Sept. 1993.

[22] J. Jin, *The Finite Element Method in Electromagnetics*: John Wiley & Sons, 2002.

[23] F. Deek and M. El-Shenawee, "Microwave Detection of Cracks in Buried Pipes Using The Complex Frequency Technique," *Applied*

Computational Electromagnetics Society (ACES) Journal, vol. 25, no. 10, pp. 894-902, Oct. 2010.

[24] B. Honarbakhsh and A. Tavakoli, "Scattering by a 2D Crack: The Meshfree Collocation Approach," *Applied Computational Electromagnetics Society (ACES) Journal*, vol. 27, no. 3, pp. 278 - 284, March 2012.

[25] M. A. Morgan and F. K. Schwering, "Mode Expansion Solution for Scattering by a Material Filled Rectangular Groove," *Progress in Electromagnetics Research (Pier)*, vol. 18, pp. 1-17, 1998.

[26] G. Bao, J. Gao, J .Lin, and W. Zhang, "Mode Matching for the Electromagnetic Scattering From Three-Dimensional Large Cavities," *IEEE Trans. Antennas Propag.*, vol. 60, no. 4, pp. 2004-2010, April 2012.

[27] A. Taflove and S. Hagness, *Computational Electrodynamics: The Finite-Difference Time-Domain Method*, Third ed: Artech House, 2005.

[28] J. C. Rautio, "The Microwave Point of View on Software Validation," *IEEE Antennas Propagat. Mag.*, vol. 38, no. 2, pp. 68-71, April 1996.

Behbod Ghalamkari was born in Tehran, Iran, on December 5, 1981. He received B.Sc. degree in Electrical Engineering from Semnan University of Semnan, Semnan, Iran, in 2005, the M.Sc. degree from the Amirkabir University of Technology (Tehran Polytechnic), Tehran, Iran, in 2007, both in electrical engineering. He is currently working toward the Ph.D. degree in electrical engineering in Amirkabir University of Technology. His main interest lies in the electromagnetic wave propagation, scattering and optimization in electromagnetic problems.

Ahad Tavakoli was born in Tehran, Iran, on March 8, 1959. He received the B.S. and M.S. degrees from the University of Kansas, Lawrence, and the Ph.D. degree from the University of Michigan, Ann Arbor, all in Electrical Engineering, in 1982, 1984, and 1991, respectively.

He is currently a Professor in the Department of Electrical Engineering at Amirkabir University of Technology. His research interests include EMC, scattering of electromagnetic waves and microstrip antennas.

Mojtaba Dehmollaian was born in Iran in 1978. He received the B.S. and M.S. degrees in electrical engineering from the University of Tehran, Tehran, Iran, in 2000 and 2002, respectively. He received the M.S. degree in applied mathematics and Ph.D. degree in electrical engineering from the University of Michigan, Ann Arbor, in 2007.

Currently, he is an Assistant Professor with the Department of Electrical and Computer Engineering, University of Tehran. His research interests are applied electromagnetics, radar remote sensing, and electromagnetic wave propagation, and scattering.